

1 **Identification and characterization of antigen-specific CD8<sup>+</sup> T cells using surface-trapped**  
2 **TNF- $\alpha$  and single-cell sequencing**

3

4 Shaheed Abdulhaqq<sup>1</sup>, Abigail B Ventura<sup>1</sup>, Jason S Reed<sup>1</sup>, Arman A Bashirova<sup>2</sup>, Katherine B  
5 Bateman<sup>1</sup>, Eric McDonald<sup>1</sup>, Helen L Wu<sup>1</sup>, Justin M Greene<sup>1</sup>, John B. Schell<sup>1</sup>, David Morrow<sup>1</sup>,  
6 Karin Wisskirchen<sup>6</sup>, Jeffrey N Martin<sup>3</sup>, Steven G Deeks<sup>4</sup>, Mary Carrington<sup>2,5</sup>, Ulrike Protzer<sup>6</sup>,  
7 Klaus Fröh<sup>1</sup>, Scott G Hansen<sup>1</sup>, Louis J Picker<sup>1</sup>, Jonah B Sacha<sup>1,7\*</sup>, Benjamin N Bimber<sup>7\*</sup>

8 \* Corresponding author. Emails: [bimber@ohsu.edu](mailto:bimber@ohsu.edu) (B.N.B.), [sacha@ohsu.edu](mailto:sacha@ohsu.edu) (J.B.S.). Phone:  
9 503-418-2755 (B.N.B.), (503)-418-2774 (J.B.S.)

10

11 <sup>1</sup> Vaccine and Gene Therapy Institute, Oregon Health and Science University, Beaverton, OR,  
12 97006, USA

13 <sup>2</sup> Basic Science Program, Frederick National Laboratory for Cancer Research, Frederick, MD  
14 21702 and Laboratory of Integrative Cancer Immunology, Center for Cancer Research, National  
15 Cancer Institute, Bethesda, MD 20892, USA

16 <sup>3</sup> Department of Epidemiology and Biostatistics, University of California, San Francisco, San  
17 Francisco, CA 94110, USA

18 <sup>4</sup> HIV/AIDS Program, Department of Medicine, University of California, San Francisco, San  
19 Francisco, CA 94110, USA

20 <sup>5</sup> Ragon Institute of Massachusetts General Hospital, Massachusetts Institute of Technology  
21 and Harvard University, Cambridge, MA 02139, USA

22 <sup>6</sup> Institute of Virology, Technical University of Munich/Helmholtz Zentrum Munich, Munich,  
23 81675, Germany

24 <sup>7</sup> Oregon National Primate Research Center, Oregon Health and Science University, Beaverton,  
25 OR, 97006, USA

26

27 Running title: Rapid identification of antigen-specific CD8<sup>+</sup> T cells

28

29 Financial Support: This work was supported by NIH R01 AI140888 and R01 AI129703 to JBS,  
30 K01 OD029804 to SA, and R01 AI059457 to KF and DOD grant W81XWH\_19\_10358 to KF.

31 This project has been funded in part with federal funds from the Frederick National Laboratory  
32 for Cancer Research, under Contract No. HHSN261200800001E. The SCOPE cohort was  
33 supported the UCSF/Gladstone Institute of Virology & Immunology CFAR (P30 AI027763) and  
34 the CFAR Network of Integrated Systems (R24 AI067039).

35 **Abstract**

36 CD8<sup>+</sup> T cells are key mediators of antiviral and antitumor immunity. The isolation and study of  
37 antigen-specific CD8<sup>+</sup> T cells, as well as mapping of their MHC restriction, has practical  
38 importance to the study of disease and the development of therapeutics. Unfortunately, most  
39 experimental approaches are cumbersome, due to the highly variable and donor-specific nature  
40 of MHC-bound peptide/TCR interactions. Here we present a novel system for rapid identification  
41 and characterization of antigen-specific CD8<sup>+</sup> T cells, particularly well-suited for samples with  
42 limited primary cells. Cells are stimulated *ex vivo* with antigen of interest, followed by live cell  
43 sorting based on surface-trapped TNF- $\alpha$ . We take advantage of major advances in single-cell  
44 sequencing to generate full-length sequence from the paired TCR alpha and beta chains from  
45 these antigen-specific cells. The paired TCR chains are cloned into retroviral vectors and used  
46 to transduce donor CD8<sup>+</sup> T cells. These TCR transductants provide a virtually unlimited  
47 experimental reagent, which can be used for further characterization, such as minimal epitope  
48 mapping or identification of MHC restriction, without depleting primary cells. We validated this  
49 system using Cytomegalovirus-specific CD8<sup>+</sup> T cells from rhesus macaques, characterizing an  
50 immunodominant Mamu-A1\*002:01-restricted epitope. We further demonstrated the utility of this  
51 system by mapping a novel HLA-A\*68:02-restricted HIV Gag epitope from an HIV-infected  
52 donor. Collectively, these data validate a new strategy to rapidly identify novel antigens and  
53 characterize antigen-specific CD8<sup>+</sup> T cells, with applications ranging from the study of infectious  
54 disease to immunotherapeutics and precision medicine.

55

56 **Key Points:**

- 57
- Surface-trapped TNF- $\alpha$  and single-cell sequencing can identify antigen specific TCRs
  - Exogenous TCR expression in donor cells allows characterization and epitope mapping
- 58

## 59 **Introduction**

60 CD8<sup>+</sup> T cells are key mediators of antiviral and antitumor immunity (1, 2). During maturation,  
61 naïve T cells undergo somatic DNA rearrangement to form a unique T cell receptor (TCR) (3, 4).  
62 This receptor is a heterodimer of two unique and variable TCR chains (most commonly alpha  
63 and beta chains), which interact with the invariant CD3 chains (5). The alpha/beta chains form a  
64 receptor that recognizes antigenic peptides presented by MHC molecules on the antigen  
65 presenting cell. The diversity of MHC/HLA genotypes across the population ensures that the  
66 identity of antigenic peptides is equally diverse and donor-specific. Determining the identity of  
67 these antigenic peptide/MHC pairs can be a laborious and expensive process (6, 7). For these  
68 reasons, the study of CD8<sup>+</sup> T cells frequently leverages a handful of well-characterized  
69 immunodominant epitopes presented by common MHC/HLA alleles, such as Mamu-A1\*001:01  
70 (A\*01)/SIV Tat SL8 in SIV-infected macaques, HLA\*B27/HIV Gag KK10 in HIV-infected  
71 humans, or HLA-A\*0201/IAV M1<sub>58-66</sub> in influenza-infected humans (8-11).

72 Characterizing the CD8<sup>+</sup> T cell response to a pathogen does not necessarily require knowing  
73 the identity of the antigenic peptides. Upon antigenic stimulation, such as antigen presenting  
74 cells (APCs) pulsed with peptide pools or virally-infected targets, activated CD8<sup>+</sup> T cells can up-  
75 regulate surface markers or secrete cytokines, including interferon gamma (IFN- $\gamma$ ) and tumor  
76 necrosis factor alpha (TNF- $\alpha$ ). Flow cytometric or ELISpot assays take advantage of these  
77 markers to identify and perform basic characterization of responding cells (12, 13). One  
78 common flow-based assay is intracellular cytokine staining (ICS), in which CD8<sup>+</sup> T cells are  
79 exposed to antigen in the presence of Brefeldin A (BFA), a compound that inhibits protein  
80 transport from the endoplasmic reticulum (ER) (14). BFA prevents cytokine secretion, trapping  
81 IFN- $\gamma$  and TNF- $\alpha$  within the cell, thereby providing a highly sensitive flow-based readout of  
82 activation (14, 15). It should be noted that ICS requires fixation and permeabilization of the cells,  
83 and therefore does not permit isolation of viable cells. If viable cells are required, staining and

84 sorting using fluorescently labeled MHC-I tetramers (or higher-order multimers), remains the  
85 gold standard (16, 17). While these tetramers can be highly specific, they are limited to  
86 previously characterized MHC/peptide specificities, making them costly to generate and limiting  
87 the utility of a given tetramer. Cytokine-capture methods provide an alternative to tetramer  
88 staining (18). One form of capture assays uses bi-specific antibodies to tether a secreted  
89 molecule, such as IFN- $\gamma$ , to the cell surface (19-21). Capture methods have the advantage of  
90 not requiring knowledge of antigenic peptides, and they can provide viable cells for downstream  
91 characterization; however, they often require species-specific reagents. An alternative cytokine  
92 capture method involves incubating CD8<sup>+</sup> T cells in the presence of TAPI-0, a metalloprotease  
93 inhibitor that blocks the activity of TNF- $\alpha$  converting enzyme (TACE) (22). TACE inhibition  
94 prevents the cleavage of TNF- $\alpha$ , thereby tethering it to the cell surface and providing a surface  
95 marker that can be used to live-sort viable cells. TCR sequencing has demonstrated that CD8<sup>+</sup>  
96 T cells sorted using surface-trapped TNF- $\alpha$  can be highly specific and sensitive (23). Sorting  
97 cells based on functional attributes, such as TNF- $\alpha$  production, may even have advantages over  
98 tetramer-staining because it identifies cells that are functional, and may identify clones with  
99 TCRs that bind with low affinity to MHC molecules (24, 25). For these reasons, while TCR  
100 sequencing has demonstrated that the set of clones identified by cytokine capture assays  
101 broadly recapitulate tetramer staining, the clonal frequencies are not expected to be identical for  
102 each method (23, 24).

103 Identification of antigen-specific TCR sequences would provide an alternative strategy to study  
104 CD8<sup>+</sup> T cells; however, the identification of TCR sequences can be extremely laborious. A  
105 productive alpha/beta TCR is comprised of two independently coded chains (26, 27).

106 Generating the sequence of the paired alpha/beta TCRs from antigen-specific CD8<sup>+</sup> T cell is  
107 most readily accomplished through single-cell sequencing (28). Single cell sequencing methods  
108 have advanced dramatically, with droplet based methods now capable of capturing

109 transcriptomic data from thousands of individual cells in a single experiment (29-31). Further,  
110 these methods have been extended to allow PCR enrichment of TCR or B cell receptor (BCR)  
111 sequences, providing near-full length sequence data (32). Once the sequence is known, the  
112 TCR alpha/beta pair can be synthesized and exogenously expressed in donor CD8<sup>+</sup> T cells (33,  
113 34). This exogenous expression has been shown to recapitulate the antigenic potential of the  
114 original cell (35, 36). Further, modifications have been published to enhance the surface  
115 expression of exogenous TCR, and prevent pairing with any endogenous TCR from the donor  
116 cells (37).

117 We reasoned that the combination of cytokine-capture, massively parallel single-cell  
118 sequencing, and exogenous TCR expression in donor cells would provide a novel system to  
119 characterize antigen specific CD8<sup>+</sup> T cells and identify antigenic peptides. This scheme is  
120 especially well suited to situations where primary cells are limited, since it only requires one  
121 round of screening and TCR identification from primary patient samples. We tested this system  
122 using Cytomegalovirus-specific CD8<sup>+</sup> T cell responses in rhesus macaques, validating the  
123 sensitivity and accuracy of this approach. We further demonstrate efficacy using cells from an  
124 HIV-infected donor, successfully mapping a novel HLA-A\*68:02-restricted HIV Gag epitope.

125

126

127

128

129

130

131

132

133

134

## 135 **Materials and Methods**

### 136 *Animals*

137 A total of 24 Indian-origin rhesus macaques were used in this study. At assignment, all study  
138 macaques were free of cercopithecine herpesvirus 1, D-type simian retrovirus, simian T-  
139 lymphotropic virus type 1, and *Mycobacterium tuberculosis*. All animals, except for the  
140 enhanced specific-pathogen free macaques, were naturally infected with rhesus CMV. All study  
141 macaques were housed at the Oregon National Primate Research Center (ONPRC) in animal  
142 biosafety level 2 rooms with autonomously controlled temperature, humidity, and lighting.  
143 Macaques were fed commercially prepared primate chow twice daily and received supplemental  
144 fresh fruit or vegetables daily. Fresh, potable water was provided via automatic water systems.  
145 Physical examinations including body weight and complete blood counts were performed at all  
146 protocol time points. Macaque care and all experimental protocols and procedures were  
147 approved by the ONPRC Institutional Animal Care and Use Committee. The ONPRC is a  
148 Category I facility. The Laboratory Animal Care and Use Program at the ONPRC is fully  
149 accredited by the American Association for Accreditation of Laboratory Animal Care and has an  
150 approved assurance (no. A3304-01) for the care and use of animals on file with the National  
151 Institutes of Health Office for Protection from Research Risks. The Institutional Animal Care and  
152 Use Committee adheres to national guidelines established in the Animal Welfare Act (7 U.S.  
153 Code, sections 2131–2159) and the *Guide for the Care and Use of Laboratory Animals, Eighth*  
154 *Edition* as mandated by the U.S. Public Health Service Policy.

155

### 156 *Human Subjects*

157 This study includes PBMC samples from a patient enrolled in the well-characterized SCOPE  
158 (Study of the Consequences of the Protease Inhibitor Era) cohort. SCOPE is an observational

159 prospective cohort based on the HIV/AIDS clinics at the Zuckerberg San Francisco General  
160 Hospital and the San Francisco Veterans Affairs Medical Center (San Francisco, CA). All  
161 subjects provided written informed consent and the parent study was approved by the UCSF  
162 Committee on Human Research. All subjects were characterized with respect to age, gender,  
163 ethnicity, HIV status (serostatus, blood CD4<sup>+</sup> and CD8<sup>+</sup> T-cell counts, plasma HIV RNA  
164 concentrations) and ART regimen.

165

### 166 *Tetramer Staining*

167 PBMC from RhCMV-infected Mamu-A1\*002:01 (Mamu-A\*02) rhesus macaques were isolated  
168 from anticoagulant-treated whole blood by Ficoll density gradient centrifugation (GE  
169 Healthcare). Tetramers for the Mamu-A\*02-restricted RhCMV IE-2<sub>313-322</sub> AN10 were provided by  
170 the NIH Tetramer Core Facility. For tetramer staining, approximately 1-2x10<sup>6</sup> cells were placed  
171 in 100 µl of RPMI 1640 (with 10% FBS). Tetramer was added at a final concentration of 100nM  
172 and cells were incubated in the dark at 37°C for 30 minutes. Subsequently, cells were stained  
173 for anti-CD3 (clone: SP34-2, Pacific Blue, BD Biosciences), anti-CD8 (clone: SK1, TruRed, BD  
174 Biosciences), anti-CD4 (clone: L200, PE-Cy7, BD Biosciences), anti-CD14 (clone M5E2, FITC,  
175 BioLegend), anti-CD16 (clone 3G8, FITC, BioLegend), and LIVE/DEAD Fixable Near Infra-Red  
176 Dead Cell Stain (Life Technologies) and were incubated for an additional 30 minutes in the dark  
177 at 4°C. Cells were then washed once with 1x PBS and fixed with 2% PFA. Sample collection  
178 was performed on LSR-II or FACSymphony instruments (BD Biosciences), and analysis was  
179 conducted with FlowJo software (Tree Star).

180

### 181 *Antigens and Antigen-Presenting Cells*

182 All peptides utilized in these studies were synthesized by Genscript. RhCMV (Genbank  
183 accession MT157325: <https://www.ncbi.nlm.nih.gov/nuccore/MT157325>) peptide pools  
184 consisted of 15mer peptides overlapping by 11 amino acids corresponding to the non-  
185 overlapping exons of RhCMV-IE1, RhCMV-IE-2 (38). Peptide pools from HIV-1 Clade B Gag  
186 were provided by the National Institutes of Health (NIH) AIDS Research and Reference Reagent  
187 Program (Germantown MD, USA). PBMC were isolated from anticoagulant-treated whole blood  
188 by Ficoll density gradient centrifugation (GE Healthcare). B-lymphoblastoid cell lines (BLCL)  
189 were generated by infecting macaque and human PBMC with herpesvirus papio or Epstein Barr  
190 virus, respectively, as previously described (39-41). Antigen-presenting cells were pulsed with  
191 peptides of interest at a final concentration of 10 $\mu$ M for 90 minutes then washed three times with  
192 warm PBS and once with warm R10 (RPMI 1640 supplemented with 10% fetal bovine serum, L-  
193 glutamine, and antibiotic/antimycotic) to remove unbound peptide before combining with  
194 effectors. The .221 cell lines expressing single HLA alleles were generated using lentiviral  
195 transduction as described (42). HLA fragments were cloned into the modified pLVX-EF1 $\alpha$ -IRES-  
196 Puro (Clontech) vector, in which EF1 $\alpha$  was replaced with the spleen focus-forming virus  
197 promoter. The expression cassette encoded ZsGreen linked via self-cleaved P2A peptide to  
198 HLA with a FLAG-tag at its N terminus. HLA-positive cells were selected using 0.25  $\mu$ g/ml  
199 puromycin.

200

#### 201 *Intracellular Cytokine Staining Assays*

202 Antigen-presenting cells were pulsed with peptides of interest at a final concentration of 10 $\mu$ M  
203 for 90 minutes, washed three times with warm PBS, and once with warm R10 (RPMI 1640  
204 supplemented with 10% fetal bovine serum, L-glutamine, and antibiotic/antimycotic) to remove  
205 unbound peptide before combining with effectors.



206 CD8<sup>+</sup> T cell responses were measured by flow cytometric ICS. PBMC, isolated CD8 $\beta$ <sup>+</sup> T cells,  
207 or CD8<sup>+</sup> T cell transductants were incubated with peptide-pulsed BLCL as described above or  
208 free peptide at a final concentration of 10 $\mu$ M, and the costimulatory molecules CD28 and CD49d  
209 (BD Biosciences) for 1 hour, followed by addition of brefeldin A (Sigma-Aldrich) for an additional  
210 8 hours. Co-stimulation with un-pulsed APCs served as background controls. Stimulated cells  
211 were stained, collected, and analyzed as previously described (43, 44). Briefly, cells were  
212 washed with 1x PBS, surface stained for 30 min, washed with PBS, fixed with 2%  
213 paraformaldehyde, permeabilized with Medium B buffer (ThermoFisher), and stained  
214 intracellularly for 1 hour. Antibodies used for ICS included: anti-CD3 (clone: SP34-2, Pacific  
215 Blue, BD Biosciences), anti-CD8 (clone: SK1, TruRed, BD Biosciences), anti-CD4 (clone: L200,  
216 PE-Cy7, BD Biosciences), anti-IFN- $\gamma$  (clone: B27, FITC, BD Biosciences), anti-TNF (clone:  
217 MAb11, APC, BD Biosciences), LIVE/DEAD Fixable Near Infra-Red Dead Cell Stain (Life  
218 Technologies) was used to assess cell viability. Sample collection was performed on an LSR-II  
219 instrument (BD Biosciences), and analysis was conducted with FlowJo software (Tree Star).

220

#### 221 *Surface-Trapped TNF- $\alpha$ Staining Assays*

222 Antigen-specific CD8<sup>+</sup> T cells were identified and viable cells sorted using surface-trapped TNF-  
223  $\alpha$  staining (23). PBMC, isolated CD8 $\beta$ <sup>+</sup> T cells, or CD8<sup>+</sup> T cell transductants were incubated  
224 with peptide-pulsed antigen-presenting cells, the co-stimulatory molecules CD28 and CD49d  
225 (BD Biosciences), anti-TNF (clone: MAb11, PE, BD Biosciences) and TAPI-0 (5 $\mu$ M final  
226 concentration, Santa Cruz Biotechnology). Cells were incubated at 37°C for 8 hours. After  
227 incubation, cells were stained anti-CD3 (clone: SP34-2, Pacific Blue, BD Biosciences), anti-CD8  
228 (clone: SK1, TruRed, BD Biosciences), anti-CD4 (clone: L200, PE-Cy7, BD Biosciences), anti-  
229 CD14 (clone: M5E2, APC, Biolegend), anti-CD69 (FN50, FITC, BioLegend), anti-CD16 (clone:  
230 3G8, APC, Biolegend), and anti-CD20 (clone: 2H7, APC, Biolegend) and LIVE/DEAD Fixable

231 Near Infra-Red Dead Cell Stain (Life Technologies) was used to assess cell viability. Antigen-  
232 specific cells were defined as TNF+/CD69+ CD8<sup>+</sup> T cell responses 2x the magnitude of the no  
233 peptide control, with the no peptide control responses below 0.5%. Viable antigen-specific cells  
234 were sorted using a FACSAria Fusion (BD Biosciences), and analysis was conducted with  
235 FlowJo software (Tree Star).

236

### 237 *ELISPOT Assay*

238 IFN- $\gamma$  ELISPOT was performed on TCR transductants, similar to previously described methods  
239 (12, 22). Briefly, 10,000 BLCL were incubated with 10  $\mu$ M of the indicated peptide(s) for 90  
240 minutes, washed 3X with 1X PBS, and then combined with 5,000-35,000 effectors. Results are  
241 reported as IFN- $\gamma$  spot-forming cells (SFCs) per  $1 \times 10^4$  effectors, following subtraction of  
242 duplicate wells with media only (negative control).

243

### 244 *Single-cell RNA-seq and TCR sequencing*

245 Viable CD8<sup>+</sup> T cells were sorted into 20 $\mu$ L chilled R10 media using a FACSAria Fusion (BD  
246 Biosciences). Sorted cells were loaded into a 10x Genomics Chromium instrument (10x  
247 Genomics) and processed using the Single Cell 5' and V(D)J Enrichment kit Version 1.1  
248 following the manufacturer's protocol. Generation of gene expression libraries was performed  
249 using manufacturer's instructions. Generation of VDJ enriched libraries followed manufacturer's  
250 instructions with the exception that macaque-specific TCR constant region primers were used in  
251 place of human-specific TCR enrichment primers. Enrichment was performed using two nested  
252 PCR reactions. The first enrichment PCR used the forward primer 5'-  
253 AATGATACGGCGACCACCGAGATCTACACTCTTCCCTACACGACGCTC-3 at a stock  
254 concentration of 1 $\mu$ M, with reverse primers targeting the alpha and beta constant regions: 5-

255 GTCTGCTGGAATAACGCTGTCC-3 (1uM stock conc.), and 5-  
256 GCGCTGATCTTTTGGGTGATGG-3 (0.5uM stock conc.). The nested PCR used the forward  
257 primer 5- AATGATACGGCGACCACCGAGATCT-3 (1uM stock conc.) and reverse primers  
258 targeting the alpha and beta constant regions: 5- ATGCACGTCAGAATCCTTGC-3 (1uM stock  
259 conc.) and 5- CAGAAGGTGGCCGAGACC-3 (0.5uM stock conc.). In both cases the  
260 concentration of the alpha constant region primer was increased relative to the beta primer to  
261 improve capture. PCR conditions for both reactions were as follows: lid temp 105°C, 98°C 0:45,  
262 12 cycles of: 98°C 0:20, 60°C 0:30, 72°C 1:00, followed by 72°C 1:00 and 4°C hold. To  
263 multiplex samples, cell hashing was used, using the MULTI-Seq lipid labeling system (45, 46).  
264 Sequence libraries were sequenced using Illumina chemistry, on either Novaseq or HiSeq  
265 instruments (Illumina).

266

### 267 *TCR Sequence Analysis*

268 Raw sequence reads for gene expression and TCR enrichment were first processed using  
269 cellranger software, version 3.1 (10x Genomics). For TCR analyses, data were aligned using a  
270 custom macaque V/J segment library, developed by our group, available in repseqio format  
271 (47). This library was provided to the cellranger vdj software. The raw clonotype calls produced  
272 by cellranger vdj were extracted from the comma-delimited outputs. Cells were demultiplexed  
273 and TCR calls were assigned to samples using custom software, made publically available  
274 through the cellhashR package (46).

275

### 276 *Generation of retroviral transduction vectors*

277 For clones of interest, near full-length V/J sequences were obtained by aligning the consensus  
278 sequences from multiple cells. The resulting consensus sequences were trimmed to the V/J

279 open reading frame. Any internal EcoRI or NotI restriction sites were altered with single  
280 nucleotide substitutions that preserved the amino acid sequence, but removed the restriction  
281 site. For each clone, the macaque TRA and TRB V/J sequences were combined *in silico* with  
282 modified murine TRA and TRB constant regions, and separated by a P2A site (37). See  
283 Supplemental Table I for the full sequence of each construct. The resulting sequences were  
284 synthesized (Genscript), digested with EcoRI and NotI, and cloned into the pMP71 retroviral  
285 vector (48). This system has been previously described for T cell transduction (48-50). Murine  
286 constant regions are used because they prevent pairing with endogenous TCR chains, and they  
287 have been modified to encode additional cysteine residues, thereby increasing the alpha/beta  
288 constant region binding affinity and thereby increasing TCR surface expression (37). This vector  
289 was used to transfect HEK293-based retroviral packaging cell line 293Vec-RD114 (provided by  
290 BioVec Pharma) using TransIT LT1 (Mirus Bio), following the manufacturer's protocol. After 24  
291 hours, the transfection reagent was replaced with fresh medium, and supernatant was  
292 harvested 24 hours later, centrifuged to remove debris, aliquoted, and frozen.

293

#### 294 *Transduction of CD8 T cells with Murinized TCR*

295 CD8<sup>+</sup> T cell-enriched PBMC were isolated from rhesus macaque PBMC utilizing a CD4 non-  
296 human primate (NHP) bead kit (Miltenyi) according to manufacturer's instructions. Isolated cells  
297 were resuspended in X-Vivo-15 medium (Lonza) supplemented with 10% FBS and 500 U/ml IL-  
298 2 (Genscript). Cells were then stimulated with a T Cell Activation/Expansion NHP Kit (Miltenyi)  
299 in accordance with manufacturer instructions. Cells were then incubated for 48 hours at 37°C.  
300 Activated T cells were separated from T cell activation kit beads by centrifugation on a ficoll (GE  
301 Healthcare) gradient. Cells were washed, resuspended in supplemented X-Vivo-15 medium,  
302 and plated in 24-well plates at 2x10<sup>6</sup> per ml.

303 RD114 TCR supernatants were thawed and centrifuged at 20,000 x g at 4°C for 1 hour on a  
304 20% sucrose (w/v) gradient. The supernatants were removed and residual volume and pellets  
305 were incubated with ViroMag beads (OzBiosciences) for 15 minutes at room temperature.  
306 Beads/RD114-pseudotyped retrovirus were then added to activated T cells and the plate was  
307 briefly spun at 1600 x g. The plate was then placed on top of the manufacturer's magnet and  
308 incubated at 37°C with 5% CO<sub>2</sub> for 15 minutes. Transduction efficiency was assessed two days  
309 post-infection by staining with anti-murine TCR β chain antibody (clone: H57-957, PE,  
310 Biolegend). Cells were then expanded for one-week before assays were performed.

311

312

313

314

315

316

317

318

319

320

321

322

323

324 **Results**

325 Rhesus cytomegalovirus-specific TCR Clonotypic Hierarchies

326 To validate whether the combination of surface-trapped TNF- $\alpha$  sorting (STTS), single-cell  
327 sequencing, and TCR transductants can rapidly identify and characterize antigen-specific CD8<sup>+</sup>  
328 T cells, we first examined responses against rhesus cytomegalovirus (RhCMV) in two rhesus  
329 macaques. Virtually all rhesus macaques are naturally infected with RhCMV at a young age,  
330 generally mounting robust CD8<sup>+</sup> T cell responses (51, 52).

331 PBMC from each animal was stimulated *ex vivo* with peptide pools for CMV intermediate/early  
332 (IE) proteins 1 and 2, along with a no peptide control, using 1 million PBMC per assay. We  
333 performed standard intracellular cytokine staining (ICS) in parallel with STTS. Incubation time  
334 and TAPI-0 concentration were determined using a separate time course experiment (Figure  
335 S1). The responses are shown in Figure 1A-B, with the magnitude of the responding cells  
336 indicated. The Rh-204C/IE-1 response was not above background (data not shown). It should  
337 be noted that while the frequency of CD69+/TNF- $\alpha$ + cells detected using STTS was consistently  
338 lower than that of the corresponding ICS assay, which may be due to inefficient or incomplete  
339 capture of TNF- $\alpha$ , sufficient CD69+/TNF- $\alpha$ + cells were detected to allow sorting. An evaluation  
340 of STTS sensitivity is shown in Figure S2.

341 Sorted cells were single-cell sequenced using the 10x Genomics platform. Prior to sorting and  
342 concurrent with fluorescent antibody staining, we labeled each PBMC sample with nucleotide-  
343 barcoded lipids (termed “cell hashing”) (45, 53). This allows samples to be pooled, which can  
344 then be multiplexed and processed using a single 10x lane. This multiplexing capability  
345 dramatically reduces the cost per sample, and is critical for throughput and feasibility of this  
346 approach. The resulting sequence data provided the TCR clonotypic hierarchies for each  
347 response (Figure 1C-D). In each case, the response to a given protein was characterized by a

348 small number of dominant clones. Critical for this system, TCR sequence data can be linked  
349 back to individual cells, thereby identifying the pairing of alpha/beta chains (Figure 1E).

### 350 Generation and Validation of Anti-CMV Transductants

351 We selected the three most common IE-2 TCR clones for further characterization. The full-  
352 length macaque V/J regions of each TCR alpha/beta pair were synthesized and cloned into a  
353 previously described retroviral expression system (48-50). In this system, the macaque V/J  
354 regions are fused to modified murine constant regions (Figure 2A). This provides two  
355 advantages: the murine constant regions prevent pairing between the exogenous and  
356 endogenous TCRs present on the donor cells, and the murine constant regions have point  
357 mutations to create additional disulfide bonds, increasing binding affinity and thereby increasing  
358 TCR surface expression (37). The complete nucleotide sequence of each TCR construct is  
359 shown in Supplemental Table I. CD8<sup>+</sup> T cells from a macaque donor were transduced with  
360 these constructs to stably express either TCR51, TCR54, or TCR55. Surface expression of  
361 exogenous TCR can be monitored using antibodies against the murine TCR $\beta$  constant region, a  
362 further advantage of this approach (Figure 2B).

363 Next, we sought to map the RhCMV epitopes recognized by each clone, using these TCR  
364 transductants. Because both animals express the high-frequency allele Mamu-A\*02, we  
365 selected a pre-existing BLCL from a Mamu-A\*02<sup>+</sup> donor (animal Rh-A02) to use for antigen  
366 presentation. We stimulated each transductant using these BLCLs pulsed with CMV IE-2  
367 overlapping 15mer pools, followed by IFN- $\gamma$  ELISPOT. For each transductant, we detected the  
368 strongest response to peptide Pool H (Figure 2C). We then performed similar experiments in  
369 which each transductant was stimulated using the same BLCLs pulsed with each of the ten  
370 individual 15mer peptides from Pool H, followed by IFN- $\gamma$  ELISPOT. All three TCR transductants  
371 responded most strongly to two overlapping 15mers, IE-2<sub>313-327</sub> and IE-2<sub>309-323</sub> (Figure 2D). To  
372 map the minimal optimal epitope, we next stimulated TCR51 and TCR54 transductants using

373 BLCLs pulsed with the overlapping 9 and 10mer peptides from this region, using decreasing  
374 concentrations, measured by IFN- $\gamma$  ELISPOT. Peptide AN10 (ATTRSLEYKN, IE-2<sub>313-322</sub>)  
375 showed the highest affinity throughout the dilution series (Figure 2E and F). Finally, in order to  
376 verify the restricting MHC-Ia allele, transductants expressing TCR51, TCR54, or non-transduced  
377 cells were incubated with a panel of APCs, each encoding a different MHC-Ia allele, pulsed with  
378 AN10 peptide (Figure 2G). Only Rh-A02 BLCL (a Mamu-A\*02+ animal), and K562s expressing  
379 Mamu-A\*02 induced a response, measured by ICS (Figure 2G). No response was detected in  
380 the control MHC-Ia negative K562 cells, the no peptide control, or in K562s expressing either  
381 Mamu-A\*01 or Mamu-B\*008:01 (Mamu-B\*08). From these data we concluded that the dominant  
382 CMV IE-2 CD8<sup>+</sup> T cells clones from both Rh-204C and Rh-200A each recognize the peptide IE-  
383 2 AN10, presented by Mamu-A\*02.

#### 384 Validation of AN10 Using Primary Cells

385 We next sought to verify whether the *in vitro* transductant results mirrored the endogenous  
386 CD8<sup>+</sup> T cells. We constructed an MHC-I tetramer using Mamu-A\*02 and AN10. We used this  
387 tetramer to stain PBMC from Rh-204C and Rh-200A (Figure 3A). Tetramer positive cells were  
388 live sorted, followed by single-cell sequencing. Tetramer sorting identified the same dominant  
389 clones, TCR51, TCR54, and TCR55, demonstrating that the *in vitro* transductant experiments  
390 identified the correct epitope. To further validate our results, PBMC from Rh-204C and Rh-200A  
391 were stimulated *ex vivo* with AN10 peptide using STTS. Responding cells were sorted and  
392 single-cell sequenced. These experiments identified the expected TCR clones (TCR51, TCR54,  
393 and TCR55), demonstrating that primary cells are capable of cytokine production following  
394 AN10 stimulation (Figure 3B). It should be noted that in this assay TCR51 was detected at a  
395 much lower frequency than that detected by tetramer sorting, with TCR55 representing a  
396 greater fraction of cytokine-producing cells. While this could represent assay-to-assay variation,  
397 it has been reported that not all tetramer positive cells have the potential to produce TNF- $\alpha$ .



398 Tetramer staining can therefore identify a superset of cells relative to TNF- $\alpha$  based detection  
399 methods (23). Of note, while the Rh-200A IE-2 response was dominated by TCR54, the minor  
400 clone CASSSRPGLPGQETQYF (denoted with \*\* in Figure 3A) was also detected in the  
401 previous IE-2 ORF STTS (Figure 1), which suggests AN10 dominates the CMV IE-2 response in  
402 this animal. Collectively, these data demonstrate that the AN10 epitope, which was identified *in*  
403 *vitro* using TCR transductants, is the biologically relevant antigen and that AN10-specific CD8 T  
404 cells represent the majority of the CMV IE-2 CD8<sup>+</sup> T cell response in both Rh-204C and Rh-  
405 200A.

406 To provide additional validation of the AN10 epitope and to measure the frequency of this  
407 response in the Oregon National Primate Research Center (ONPRC) colony, we screened three  
408 additional cohorts: RhCMV+/Mamu-A\*02+ animals, RhCMV+/Mamu-A\*02- animals, and  
409 RhCMV-/Mamu-A\*02+ animals. The latter were selected from the ONPRC Enhanced Specific  
410 Pathogen Free (SPF) colony, and have been verified to be RhCMV-negative (23). As expected,  
411 all RhCMV+ animals had a robust ELISPOT response to CMV lysate, relative to RhCMV-  
412 animals (Figure 3C). When stimulated with AN10 peptide, only PBMC from RhCMV+/Mamu-  
413 A\*02+ animals responded, as would be expected for an epitope restricted by Mamu\*A\*02. In  
414 addition to validating our system as a rapid method for epitope identification, it is worth noting  
415 that virtually all Mamu-A\*02+ animals we tested (8/9) responded to AN10. Because such a high  
416 fraction of Mamu-A\*02+ animals mount this response, it may be of experimental interest either  
417 in the study of RhCMV, or as a control CD8<sup>+</sup> T cell response for use in other disease studies.

#### 418 Identification, Characterization, and Validation of a novel HIV Gag Response

419 We next turned to an HIV-infected human donor, representing a sample with limited primary  
420 cells. Following a similar strategy as the macaque experiments, we initially stimulated PBMC *ex*  
421 *vivo* with HIV-1 Clade B Gag peptide pools, followed by IFN- $\gamma$  ELISPOT (Figure 4A-B). These  
422 experiments consumed 1 million primary PBMC per pool. While multiple peptide pools produced

423 responses above background, we selected Pool E for further characterization. As before, we  
424 performed STTS using 1 million PBMC, live-sorted the responding cells, and performed single-  
425 cell sequencing (Figure 4B). The TCR repertoire to this peptide pool was dominated by one  
426 major clone: 1247-TCR-1 (Figure 4C-D). We synthesized this clone and inserted it into the  
427 same expression vector as before, expressing the human V/J segments fused to modified  
428 murine constant regions (Figure 2A). This construct was used to generate retrovirus and  
429 transduce CD8<sup>+</sup> T cells from an HIV-naïve donor (Figure 4E). We next sought to map the  
430 minimal epitope for this clone, following the same approach as the rhesus macaque  
431 experiments. TCR transductants expressing 1247-TCR-1 were stimulated *in vitro* using  
432 autologous BLCL peptide-pulsed with the individual 15mer peptides from Gag Pool E,  
433 identifying Gag<sub>165-179</sub> (SA15) as the strongest response (Figure 4F). We next performed two sets  
434 of experiments in parallel. To identify the minimal optimal epitope, we stimulated 1247-TCR-1  
435 transductants with autologous BLCL pulsed with the 9-10mer peptides overlapping SA15,  
436 followed by IFN- $\gamma$  ELISPOT (Figure 4G). This identified EL9 (EVIPMFSAL, Gag<sub>167-175</sub>) as the  
437 minimal optimal peptide. Finally, we sought to identify the restricting HLA allele. We performed  
438 flow cytometric ICS with a panel of MHC-I null .221 cells, with each expressing a single HLA  
439 allele present in the donor: HLA-A\*32:01, HLA-A\*68:02, HLA-B\*39:10, HLA-B\*53:01, HLA-  
440 Cw\*04:01, and HLA-Cw\*14:03. These APCs were pulsed with the SA15 peptide and incubated  
441 with 1247-TCR-1 transductants, followed by ICS (Figure 4H). The only APCs to elicit a response  
442 above background were cells expressing HLA-A\*68:02, identifying HLA-A\*68:02 as the  
443 presenting HLA allele. We subsequently peptide pulsed .221s expressing HLA-A\*68:02 with  
444 either SA15 or the minimal epitope EL9, followed by incubation with 1247-TCR-1 transductants  
445 and ICS (Figure S3). As expected, the minimal optimal EL9 peptide elicited a nearly 2-fold  
446 higher response.

447 Of interest, the EL9 peptide has been described in prior studies as an HLA-A\*26-restricted  
448 response, and this peptide has been included in a commonly used ELISPOT screening panel  
449 (10, 54-58). To test whether 1247-TCR-1 could recognize EL9 bound by HLA-A\*26, we  
450 generated .221 cells expressing either HLA-A\*68:02 or HLA-A\*26:01. These APCs were pulsed  
451 with EL9 peptide and incubated with 1247-TCR-1 transductants, followed by ICS (Figure S3).  
452 The HLA-A\*26:01 expressing cells did not elicit a response above background, indicating that  
453 even if EL9 can be presented by HLA-A\*26:01, it is not recognized by 1247-TCR-1. Our data  
454 nonetheless demonstrate this Gag epitope can be presented by multiple HLA alleles.

455

456

457

458

459

460

461

462

463

464

465

466

467

## 468 **Discussion**

469 Here we present a novel scheme to characterize antigen-specific CD8<sup>+</sup> T cells and their cognate  
470 MHC antigens. This system combines three components: 1) high sensitivity TNF- $\alpha$  capture to  
471 identify and isolate viable antigen-specific cells, 2) massively parallel single-cell resolution  
472 sequencing to identify the complete clonotypic hierarchy of each response, and 3) exogenous  
473 expression of the TCR alpha/beta pair on donor cells. The latter produces a nearly unlimited  
474 experimental reagent that can be used for *in vitro* validation and characterization, without  
475 depleting primary cells. We demonstrate this system accurately identifies and characterizes  
476 antigen specific CD8<sup>+</sup> T cells in both CMV-infected rhesus macaques and an HIV-infected  
477 donor, identifying the antigenic peptides and restricting MHC alleles for each. We validated our  
478 results using primary cells, demonstrating the *in vitro* system recapitulates endogenous  
479 TCR/MHC interactions.

480 This system has a wide range of applications. It provides a clear advantage whenever  
481 patient/donor samples are limited. This approach requires as little as one experiment with  
482 primary cells: the STTS screen to identify antigen-specific TCR sequences. Even when samples  
483 are not limited, such as most studies using animal models, the transductant system may have  
484 benefits. For example, it could facilitate epitope mapping when the host response is weak or  
485 rare. In some contexts, the primary CD8<sup>+</sup> T cell response to a given antigen may be difficult to  
486 culture *in vitro*, such as the terminally differentiated CD8<sup>+</sup> T cell responses elicited by CMV  
487 vaccine vectors (39, 43). The identification of the TCR sequences, followed by expression in  
488 transductants may facilitate study of these T cells. The rapid generation and characterization of  
489 patient-specific T cell responses and their cognate antigens has clear applications for the  
490 creation of personalized immunotherapeutics as well.

491 The system is premised on CD8<sup>+</sup> T cell antigen specificity being conferred nearly exclusively  
492 through the TCR and cognate MHC-bound peptide. Exogenous expression of the specific TCR

493  $\alpha/\beta$  pair on donor cells is generally sufficient for antigenic recognition, as we demonstrate in this  
494 study and has been previously published (35, 37, 59-62). There are nonetheless examples of  
495 other receptors and signaling pathways that modulate CD8<sup>+</sup> T cell specificity and activation (63,  
496 64). Potentially interesting extensions of the system we present in this study could involve  
497 careful selection or experimental manipulation of the donor CD8<sup>+</sup> T cells, either to control the  
498 genetic background, or to perform overexpression or knock-out of other signaling molecules.  
499 Together, this study validates a novel system to rapidly identify CD8<sup>+</sup> T cells and their  
500 peptide/MHC antigens. We demonstrate that limited experiments with primary cells can  
501 accurately identify the TCR sequences of antigen-specific CD8<sup>+</sup> T cells, these sequences can  
502 be cloned into donor cells to recapitulate antigen specificity of the primary cells, and this *in vitro*  
503 system provides a surrogate to accurately characterize the primary CD8<sup>+</sup> T cell response. This  
504 scheme is well suited to any situation where primary cells are rare or not amenable to *ex vivo*  
505 functional studies, with a range of practical applications.

506

## 507 **Acknowledgements**

508 We thank Dr. Chris McGinnis for generously providing MULTI-seq barcoded lipids. The content  
509 of this publication does not necessarily reflect the views or policies of the Department of Health  
510 and Human Services, nor does mention of trade names, commercial products, or organizations  
511 imply endorsement by the U.S. Government.

512

## 513 **Figure Legends**

514 Figure 1. Identification of RhCMV-specific CD8<sup>+</sup> T Cell Clonotypes. A-B) PBMCs from two  
515 RhCMV+ rhesus macaques were stimulated *ex vivo* with 15mer peptide pools for either CMV

516 IE-1 or IE-2, measuring using ICS (top) or STTS (bottom). The Rh-204C IE-1 response was not  
517 above background (data not shown). C-D) CD69+/TNF- $\alpha$ + cells were live-sorted from each  
518 response, followed by single-cell sequencing. Pie charts indicate the TCR clonotypic hierarchies  
519 of each response. E) Table shows the V/J usage and CDR3 sequence for the paired alpha/beta  
520 chains of the four most common TCR clonotypes. The identity of the TRBD segment for TCR55  
521 could not be unambiguously determined from the 9-NT region between the V- and J-segments.

522

523 Figure 2. Characterization of RhCMV-specific TCRs using transductants. A) Schematic of the  
524 chimeric macaque V/J, murine constant region (“murinized”) TCR receptor, B) Representative  
525 flow plot of CD8<sup>+</sup> T cells from a donor macaque, with or without transduction of TCR54,  
526 illustrating the detection of surface murine TCR $\beta$  in transduced cells. C) Transductants  
527 expressing TCR51 (black), TCR54 (blue), or TCR55 (red) were incubated with BLCL pulsed  
528 with the indicated 15mer IE-2 peptide pools, followed by IFN- $\gamma$  ELISPOT. Bars indicate the spot  
529 forming cells per  $5 \times 10^4$  cells, after background subtraction. D) Similar graph as C showing  
530 transductants stimulated with the ten individual 15mer peptides from IE-2 Pool H. E-F) Peptide  
531 titration experiments were performed to determine the minimal/optimal peptide sequence, using  
532 overlapping 9-10mer peptides spanning IE-2 residues 313-322. BLCLs were pulsed with each of  
533 the peptides indicated in F, at varying concentrations, followed by incubation with transductants  
534 expressing either TCR51 (E) or TCR54 (F). Graphs indicate the SFC per  $5 \times 10^4$  cells, measured  
535 by IFN- $\gamma$  ELISPOT. G) Transductants expressing either TCR51 (black), TCR54 (blue), or non-  
536 transduced (green) were incubated with the indicated APCs, pulsed with AN10 peptide (IE-2<sub>313-322</sub>).  
537 Rh-A02 BLCL is from a Mamu-A\*02 positive animal. No MHC-I denotes the parent MHC-  
538 null K562 cells. A\*01, A\*02 and B\*08 denote K562 cell lines expressing the indicated MHC-Ia  
539 allele. Graph indicates the percentage of murine TCR $\beta$ + cells positive for TNF- $\alpha$  and IFN- $\gamma$ ,  
540 measured by flow cytometric ICS.

541

542 Figure 3. Ex vivo validation of IE-2 AN10. A) MHC-tetramers were folded using Mamu-A\*02 and  
543 IE-2 AN10, and then used to stain PBMC from Rh-204C and Rh-200A. Flow plots indicate the  
544 fraction of CD8<sup>+</sup> T cells stained by AN10 tetramers for each animal. The tetramer-positive cells  
545 were live sorted, followed by single-cell sequencing. Pie charts indicate the clonotypic  
546 hierarchies for each, demonstrating that the clones previously identified by IE-1/2 ORF stims are  
547 present. B) PBMC from Rh-204C and Rh-200A were stimulated *ex vivo* with AN10 peptide,  
548 followed by STTS. Pie charts indicate the clonotypic hierarchies, demonstrating that primary  
549 cells stimulated with AN10 recapitulate the transductant experiments. C) To further validate the  
550 AN10 response, and to evaluate its prevalence in the broader rhesus macaque population, we  
551 performed IFN- $\gamma$  ELISPOT using cells using animals in three groups: RhCMV-/Mamu-A\*02+,  
552 RhCMV+/Mamu-A\*02-, and RhCMV+/Mamu-A\*02+. Cells were stimulated with either CMV  
553 lysate (left), or AN10 peptide (right). Graphs indicate spot forming cells per  $5 \times 10^4$  cells (\*,  $p \leq$   
554 0.05; \*\*,  $p \leq 0.01$ ; \*\*\*,  $p \leq 0.001$ ).

555

556 Figure 4. Identification and characterization of a novel HIV Gag epitope. A) PBMCs from an  
557 HIV-infected donor, SCOPE 1247, were stimulated *ex vivo* with HIV Gag 15mer peptide pools.  
558 Graph indicates the frequency of responding cells, measured by IFN- $\gamma$  ELISPOT. Dotted line  
559 indicates the limit of quantitation (LOQ; 50 SFC per  $10^5$  CD8<sup>+</sup> T cells). B) Flow plot for STTS  
560 using SCOPE 1247 PBMCs, pulsed with HIV-1 Gag Clade B Pool E. The CD69+/TNF- $\alpha$ + cells  
561 were live cell sorted, followed by single cell sequencing. C) Pie chart indicates the TCR  
562 clonotypic hierarchy of CD8 T cells activated by Pool E peptide, demonstrating one major clone,  
563 1247-TCR-1, comprises the majority of the response. D) Table shows the paired alpha/beta  
564 chains from clone 1247-TCR-1. E) The alpha/beta chains from 1247-TCR-1 were synthesized  
565 and used to transduce donor CD8<sup>+</sup> T cells. The flow plot shows the fraction of cells stained for

566 murine TCR $\beta$ , indicating cell surface expression of exogenous 1247-TCR-1. F) IFN- $\gamma$  ELISPOT  
567 was performed using 1247-TCR-1 transductants stimulated with autologous BLCL, pulsed with  
568 each of the peptides comprising HIV Gag Pool E (LOQ = 5 SFC per 10<sup>4</sup> cells). The strongest  
569 response was detected from Gag<sub>165-179</sub> (SA15). G) ELISPOT was performed using autologous  
570 BLCL pulsed with the indicated 9 and 10mer peptides, which overlap SA15. The strongest  
571 response was detected from EVIPMFSAL (EL9). H) To determine HLA-restriction, 1247-TCR-1  
572 transductants were incubated with .221 cell lines individually expressing each of the HLA alleles  
573 encoded by the patient, pulsed with SA15 peptide. Cells expressing HLA-A\*68:02 were the only  
574 APCs that produced a response above background, measured by ICS.

575

## 576 Literature Cited

- 577 1. Appay, V., D. C. Douek, and D. A. Price. 2008. CD8+ T cell efficacy in vaccination and disease. *Nat*  
578 *Med* 14: 623-628.
- 579 2. Schreiber, R. D., L. J. Old, and M. J. Smyth. 2011. Cancer immunoediting: integrating immunity's  
580 roles in cancer suppression and promotion. *Science* 331: 1565-1570.
- 581 3. Turner, S. J., P. C. Doherty, J. McCluskey, and J. Rossjohn. 2006. Structural determinants of T-cell  
582 receptor bias in immunity. *Nat Rev Immunol* 6: 883-894.
- 583 4. Siggs, O. M., L. E. Makaroff, and A. Liston. 2006. The why and how of thymocyte negative  
584 selection. *Curr Opin Immunol* 18: 175-183.
- 585 5. Gras, S., S. R. Burrows, S. J. Turner, A. K. Sewell, J. McCluskey, and J. Rossjohn. 2012. A structural  
586 voyage toward an understanding of the MHC-I-restricted immune response: lessons learned and  
587 much to be learned. *Immunol Rev* 250: 61-81.
- 588 6. Sharma, G., and R. A. Holt. 2014. T-cell epitope discovery technologies. *Hum Immunol* 75: 514-  
589 519.
- 590 7. Dornmair, K., E. Meinl, and R. Hohlfeld. 2009. Novel approaches for identifying target antigens  
591 of autoreactive human B and T cells. *Semin Immunopathol* 31: 467-477.
- 592 8. Boon, A. C., G. de Mutsert, Y. M. Graus, R. A. Fouchier, K. Sintnicolaas, A. D. Osterhaus, and G. F.  
593 Rimmelzwaan. 2002. The magnitude and specificity of influenza A virus-specific cytotoxic T-  
594 lymphocyte responses in humans is related to HLA-A and -B phenotype. *J Virol* 76: 582-590.
- 595 9. McMichael, A. J., F. M. Gotch, and J. Rothbard. 1986. HLA B37 determines an influenza A virus  
596 nucleoprotein epitope recognized by cytotoxic T lymphocytes. *J Exp Med* 164: 1397-1406.
- 597 10. Altfeld, M., E. T. Kalife, Y. Qi, H. Streeck, M. Lichterfeld, M. N. Johnston, N. Burgett, M. E. Swartz,  
598 A. Yang, G. Alter, X. G. Yu, A. Meier, J. K. Rockstroh, T. M. Allen, H. Jessen, E. S. Rosenberg, M.  
599 Carrington, and B. D. Walker. 2006. HLA Alleles Associated with Delayed Progression to AIDS  
600 Contribute Strongly to the Initial CD8(+) T Cell Response against HIV-1. *PLoS Med* 3: e403.



- 601 11. Goulder, P. J., R. E. Phillips, R. A. Colbert, S. McAdam, G. Ogg, M. A. Nowak, P. Giangrande, G.  
602 Luzzi, B. Morgan, A. Edwards, A. J. McMichael, and S. Rowland-Jones. 1997. Late escape from an  
603 immunodominant cytotoxic T-lymphocyte response associated with progression to AIDS. *Nat*  
604 *Med* 3: 212-217.
- 605 12. Freer, G., and L. Rindi. 2013. Intracellular cytokine detection by fluorescence-activated flow  
606 cytometry: basic principles and recent advances. *Methods* 61: 30-38.
- 607 13. Newell, E. W., and W. Lin. 2014. High-dimensional analysis of human CD8(+) T cell phenotype,  
608 function, and antigen specificity. *Curr Top Microbiol Immunol* 377: 61-84.
- 609 14. Waldrop, S. L., C. J. Pitcher, D. M. Peterson, V. C. Maino, and L. J. Picker. 1997. Determination of  
610 antigen-specific memory/effector CD4+ T cell frequencies by flow cytometry: evidence for a  
611 novel, antigen-specific homeostatic mechanism in HIV-associated immunodeficiency. *J Clin*  
612 *Invest* 99: 1739-1750.
- 613 15. Hansen, S. G., J. C. Ford, M. S. Lewis, A. B. Ventura, C. M. Hughes, L. Coyne-Johnson, N. Whizin,  
614 K. Oswald, R. Shoemaker, T. Swanson, A. W. Legasse, M. J. Chiuchiolo, C. L. Parks, M. K. Axthelm,  
615 J. A. Nelson, M. A. Jarvis, M. Piatak, Jr., J. D. Lifson, and L. J. Picker. 2011. Profound early control  
616 of highly pathogenic SIV by an effector memory T-cell vaccine. *Nature* 473: 523-527.
- 617 16. Altman, J. D., P. A. Moss, P. J. Goulder, D. H. Barouch, M. G. McHeyzer-Williams, J. I. Bell, A. J.  
618 McMichael, and M. M. Davis. 1996. Phenotypic analysis of antigen-specific T lymphocytes.  
619 *Science* 274: 94-96.
- 620 17. Wooldridge, L., A. Lissina, D. K. Cole, H. A. van den Berg, D. A. Price, and A. K. Sewell. 2009.  
621 Tricks with tetramers: how to get the most from multimeric peptide-MHC. *Immunology* 126:  
622 147-164.
- 623 18. Campbell, J. D. 2003. Detection and enrichment of antigen-specific CD4+ and CD8+ T cells based  
624 on cytokine secretion. *Methods* 31: 150-159.
- 625 19. Brosterhus, H., S. Brings, H. Leyendeckers, R. A. Manz, S. Miltenyi, A. Radbruch, M.  
626 Assenmacher, and J. Schmitz. 1999. Enrichment and detection of live antigen-specific CD4(+) and  
627 CD8(+) T cells based on cytokine secretion. *Eur J Immunol* 29: 4053-4059.
- 628 20. Douek, D. C., J. M. Brenchley, M. R. Betts, D. R. Ambrozak, B. J. Hill, Y. Okamoto, J. P. Casazza, J.  
629 Kuruppu, K. Kunstman, S. Wolinsky, Z. Grossman, M. Dybul, A. Oxenius, D. A. Price, M. Connors,  
630 and R. A. Koup. 2002. HIV preferentially infects HIV-specific CD4+ T cells. *Nature* 417: 95-98.
- 631 21. Lichterfeld, M., X. G. Yu, M. T. Waring, S. K. Mui, M. N. Johnston, D. Cohen, M. M. Addo, J.  
632 Zaunders, G. Alter, E. Pae, D. Strick, T. M. Allen, E. S. Rosenberg, B. D. Walker, and M. Altfeld.  
633 2004. HIV-1-specific cytotoxicity is preferentially mediated by a subset of CD8(+) T cells  
634 producing both interferon-gamma and tumor necrosis factor-alpha. *Blood* 104: 487-494.
- 635 22. Crowe, P. D., B. N. Walter, K. M. Mohler, C. Otten-Evans, R. A. Black, and C. F. Ware. 1995. A  
636 metalloprotease inhibitor blocks shedding of the 80-kD TNF receptor and TNF processing in T  
637 lymphocytes. *J Exp Med* 181: 1205-1210.
- 638 23. Haney, D., M. F. Quigley, T. E. Asher, D. R. Ambrozak, E. Gostick, D. A. Price, D. C. Douek, and M.  
639 R. Betts. 2011. Isolation of viable antigen-specific CD8+ T cells based on membrane-bound  
640 tumor necrosis factor (TNF)-alpha expression. *J Immunol Methods* 369: 33-41.
- 641 24. Goepfert, P. A., A. Bansal, B. H. Edwards, G. D. Ritter, Jr., I. Tellez, S. A. McPherson, S. Sabbaj,  
642 and M. J. Mulligan. 2000. A significant number of human immunodeficiency virus epitope-  
643 specific cytotoxic T lymphocytes detected by tetramer binding do not produce gamma  
644 interferon. *J Virol* 74: 10249-10255.
- 645 25. Chattopadhyay, P. K., J. J. Melenhorst, K. Ladell, E. Gostick, P. Scheinberg, A. J. Barrett, L.  
646 Wooldridge, M. Roederer, A. K. Sewell, and D. A. Price. 2008. Techniques to improve the direct  
647 ex vivo detection of low frequency antigen-specific CD8+ T cells with peptide-major  
648 histocompatibility complex class I tetramers. *Cytometry A* 73: 1001-1009.

- 649 26. Rosati, E., C. M. Dowds, E. Liaskou, E. K. K. Henriksen, T. H. Karlsen, and A. Franke. 2017.  
650 Overview of methodologies for T-cell receptor repertoire analysis. *BMC Biotechnol* 17: 61.
- 651 27. Lin, H., Y. Peng, X. Chen, Y. Liang, G. Tian, and J. Yang. 2020. T Cell Receptor Repertoire  
652 Sequencing. *Methods Mol Biol* 2204: 3-12.
- 653 28. Gupta, S., R. Witas, A. Voigt, T. Semenova, and C. Q. Nguyen. 2020. Single-Cell Sequencing of T  
654 cell Receptors: A Perspective on the Technological Development and Translational Application.  
655 *Adv Exp Med Biol* 1255: 29-50.
- 656 29. Macosko, E. Z., A. Basu, R. Satija, J. Nemesh, K. Shekhar, M. Goldman, I. Tirosh, A. R. Bialas, N.  
657 Kamitaki, E. M. Martersteck, J. J. Trombetta, D. A. Weitz, J. R. Sanes, A. K. Shalek, A. Regev, and  
658 S. A. McCarroll. 2015. Highly Parallel Genome-wide Expression Profiling of Individual Cells Using  
659 Nanoliter Droplets. *Cell* 161: 1202-1214.
- 660 30. See, P., J. Lum, J. Chen, and F. Ginhoux. 2018. A Single-Cell Sequencing Guide for Immunologists.  
661 *Front Immunol* 9: 2425.
- 662 31. Zheng, G. X., J. M. Terry, P. Belgrader, P. Ryvkin, Z. W. Bent, R. Wilson, S. B. Zivaldo, T. D.  
663 Wheeler, G. P. McDermott, J. Zhu, M. T. Gregory, J. Shuga, L. Montesclaros, J. G. Underwood, D.  
664 A. Masquelier, S. Y. Nishimura, M. Schnall-Levin, P. W. Wyatt, C. M. Hindson, R. Bharadwaj, A.  
665 Wong, K. D. Ness, L. W. Beppu, H. J. Deeg, C. McFarland, K. R. Loeb, W. J. Valente, N. G. Ericson,  
666 E. A. Stevens, J. P. Radich, T. S. Mikkelsen, B. J. Hindson, and J. H. Bielas. 2017. Massively parallel  
667 digital transcriptional profiling of single cells. *Nat Commun* 8: 14049.
- 668 32. Phetsouphanh, C., J. J. Zaunders, and A. D. Kelleher. 2015. Detecting Antigen-Specific T Cell  
669 Responses: From Bulk Populations to Single Cells. *Int J Mol Sci* 16: 18878-18893.
- 670 33. Schumacher, T. N. 2002. T-cell-receptor gene therapy. *Nat Rev Immunol* 2: 512-519.
- 671 34. Kershaw, M. H., M. W. Teng, M. J. Smyth, and P. K. Darcy. 2005. Supernatural T cells: genetic  
672 modification of T cells for cancer therapy. *Nat Rev Immunol* 5: 928-940.
- 673 35. Zhao, Y., Z. Zheng, P. F. Robbins, H. T. Khong, S. A. Rosenberg, and R. A. Morgan. 2005. Primary  
674 human lymphocytes transduced with NY-ESO-1 antigen-specific TCR genes recognize and kill  
675 diverse human tumor cell lines. *J Immunol* 174: 4415-4423.
- 676 36. Leisegang, M., B. Engels, P. Meyerhuber, E. Kieback, D. Sommermeyer, S. A. Xue, S. Reuss, H.  
677 Stauss, and W. Uckert. 2008. Enhanced functionality of T cell receptor-redirected T cells is  
678 defined by the transgene cassette. *J Mol Med (Berl)* 86: 573-583.
- 679 37. Cohen, C. J., Y. Zhao, Z. Zheng, S. A. Rosenberg, and R. A. Morgan. 2006. Enhanced antitumor  
680 activity of murine-human hybrid T-cell receptor (TCR) in human lymphocytes is associated with  
681 improved pairing and TCR/CD3 stability. *Cancer Res* 66: 8878-8886.
- 682 38. Cicin-Sain, L., A. W. Sylwester, S. I. Hagen, D. C. Siess, N. Currier, A. W. Legasse, M. B. Fischer, C.  
683 W. Koudelka, M. K. Axthelm, J. Nikolich-Zugich, and L. J. Picker. 2011. Cytomegalovirus-specific T  
684 cell immunity is maintained in immunosenescent rhesus macaques. *J Immunol* 187: 1722-1732.
- 685 39. Hansen, S. G., J. B. Sacha, C. M. Hughes, J. C. Ford, B. J. Burwitz, I. Scholz, R. M. Gilbride, M. S.  
686 Lewis, A. N. Gilliam, A. B. Ventura, D. Malouli, G. Xu, R. Richards, N. Whizin, J. S. Reed, K. B.  
687 Hammond, M. Fischer, J. M. Turner, A. W. Legasse, M. K. Axthelm, P. T. Edlefsen, J. A. Nelson, J.  
688 D. Lifson, K. Fruh, and L. J. Picker. 2013. Cytomegalovirus vectors violate CD8+ T cell epitope  
689 recognition paradigms. *Science* 340: 1237874.
- 690 40. Voss, G., S. Nick, C. Stahl-Hennig, K. Ritter, and G. Hunsmann. 1992. Generation of macaque B  
691 lymphoblastoid cell lines with simian Epstein-Barr-like viruses: transformation procedure,  
692 characterization of the cell lines and occurrence of simian foamy virus. *J Virol Methods* 39: 185-  
693 195.
- 694 41. Sugden, B., and W. Mark. 1977. Clonal transformation of adult human leukocytes by Epstein-  
695 Barr virus. *J Virol* 23: 503-508.

- 696 42. Garcia-Beltran, W. F., A. Holzemer, G. Martrus, A. W. Chung, Y. Pacheco, C. R. Simoneau, M.  
697 Rucevic, P. A. Lamothe-Molina, T. Pertel, T. E. Kim, H. Dugan, G. Alter, J. Dechanet-Merville, S.  
698 Jost, M. Carrington, and M. Altfeld. 2016. Open conformers of HLA-F are high-affinity ligands of  
699 the activating NK-cell receptor KIR3DS1. *Nat Immunol* 17: 1067-1074.
- 700 43. Hansen, S. G., H. L. Wu, B. J. Burwitz, C. M. Hughes, K. B. Hammond, A. B. Ventura, J. S. Reed, R.  
701 M. Gilbride, E. Ainslie, D. W. Morrow, J. C. Ford, A. N. Selseth, R. Pathak, D. Malouli, A. W.  
702 Legasse, M. K. Axthelm, J. A. Nelson, G. M. Gillespie, L. C. Walters, S. Brackenridge, H. R. Sharpe,  
703 C. A. Lopez, K. Fruh, B. T. Korber, A. J. McMichael, S. Gnanakaran, J. B. Sacha, and L. J. Picker.  
704 2016. Broadly targeted CD8(+) T cell responses restricted by major histocompatibility complex E.  
705 *Science* 351: 714-720.
- 706 44. Abdulhaqq, S. A., H. Wu, J. B. Schell, K. B. Hammond, J. S. Reed, A. W. Legasse, M. K. Axthelm, B.  
707 S. Park, A. Asokan, K. Fruh, S. G. Hansen, L. J. Picker, and J. B. Sacha. 2019. Vaccine-Mediated  
708 Inhibition of the Transporter Associated with Antigen Processing Is Insufficient To Induce Major  
709 Histocompatibility Complex E-Restricted CD8(+) T Cells in Nonhuman Primates. *J Virol* 93.
- 710 45. McGinnis, C. S., D. M. Patterson, J. Winkler, D. N. Conrad, M. Y. Hein, V. Srivastava, J. L. Hu, L. M.  
711 Murrow, J. S. Weissman, Z. Werb, E. D. Chow, and Z. J. Gartner. 2019. MULTI-seq: sample  
712 multiplexing for single-cell RNA sequencing using lipid-tagged indices. *Nat Methods* 16: 619-626.
- 713 46. Boggy, G., Bimber BN. 2021. cellhashR: An R package designed to demultiplex cell hashing data.  
714 <https://github.com/bimberlab/cellhashr>
- 715 47. Bimber, B. 2021. Rhesus macaque V/J segment library.  
716 <https://github.com/bimberlab/internal/library>
- 717 48. Engels, B., H. Cam, T. Schuler, S. Indraccolo, M. Gladow, C. Baum, T. Blankenstein, and W.  
718 Uckert. 2003. Retroviral vectors for high-level transgene expression in T lymphocytes. *Hum Gene*  
719 *Ther* 14: 1155-1168.
- 720 49. Wisskirchen, K., K. Metzger, S. Schreiber, T. Asen, L. Weigand, C. Dargel, K. Witter, E. Kieback, M.  
721 F. Sprinzl, W. Uckert, M. Schiemann, D. H. Busch, A. M. Krackhardt, and U. Protzer. 2017.  
722 Isolation and functional characterization of hepatitis B virus-specific T-cell receptors as new  
723 tools for experimental and clinical use. *PLoS One* 12: e0182936.
- 724 50. Wisskirchen, K., J. Kah, A. Malo, T. Asen, T. Volz, L. Allweiss, J. M. Wettengel, M. Lutgehetmann,  
725 S. Urban, T. Bauer, M. Dandri, and U. Protzer. 2019. T cell receptor grafting allows virological  
726 control of Hepatitis B virus infection. *J Clin Invest* 129: 2932-2945.
- 727 51. Powers, C., and K. Fruh. 2008. Rhesus CMV: an emerging animal model for human CMV. *Med*  
728 *Microbiol Immunol* 197: 109-115.
- 729 52. Pomplun, N. L., L. Vosler, K. L. Weisgrau, J. Furlott, A. M. Weiler, H. M. Abdelaal, D. T. Evans, D. I.  
730 Watkins, T. Matano, P. J. Skinner, T. C. Friedrich, and E. G. Rakasz. 2021. Immunophenotyping of  
731 Rhesus CMV-Specific CD8 T-Cell Populations. *Cytometry A* 99: 278-288.
- 732 53. Stoeckius, M., S. Zheng, B. Houck-Loomis, S. Hao, B. Z. Yeung, W. M. Mauck, 3rd, P. Smibert, and  
733 R. Satija. 2018. Cell Hashing with barcoded antibodies enables multiplexing and doublet  
734 detection for single cell genomics. *Genome Biol* 19: 224.
- 735 54. Feeney, M. E., Y. Tang, K. A. Roosevelt, A. J. Leslie, K. McIntosh, N. Karthas, B. D. Walker, and P.  
736 J. Goulder. 2004. Immune escape precedes breakthrough human immunodeficiency virus type 1  
737 viremia and broadening of the cytotoxic T-lymphocyte response in an HLA-B27-positive long-  
738 term-nonprogressing child. *J Virol* 78: 8927-8930.
- 739 55. Pereyra, F., D. Heckerman, J. M. Carlson, C. Kadie, D. Z. Soghoian, D. Karel, A. Goldenthal, O. B.  
740 Davis, C. E. DeZiel, T. Lin, J. Peng, A. Piechocka, M. Carrington, and B. D. Walker. 2014. HIV  
741 control is mediated in part by CD8+ T-cell targeting of specific epitopes. *J Virol* 88: 12937-12948.
- 742 56. Harari, A., C. Cellera, F. Bellutti Enders, J. Kostler, L. Codarri, G. Tapia, O. Boyman, E. Castro, S.  
743 Gaudieri, I. James, M. John, R. Wagner, S. Mallal, and G. Pantaleo. 2007. Skewed association of

744 polyfunctional antigen-specific CD8 T cell populations with HLA-B genotype. *Proc Natl Acad Sci U*  
745 *S A* 104: 16233-16238.

746 57. Goulder, P., C. Conlon, K. McLntyre, and A. McMichael. 1996. Identification of a novel human  
747 leukocyte antigen A26-restricted epitope in a conserved region of Gag. *AIDS* 10: 1441-1443.

748 58. Satoh, M., Y. Takamiya, S. Oka, K. Tokunaga, and M. Takiguchi. 2005. Identification and  
749 characterization of HIV-1-specific CD8+ T cell epitopes presented by HLA-A\*2601. *Vaccine* 23:  
750 3783-3790.

751 59. Hedrick, S. M., D. I. Cohen, E. A. Nielsen, and M. M. Davis. 1984. Isolation of cDNA clones  
752 encoding T cell-specific membrane-associated proteins. *Nature* 308: 149-153.

753 60. Yanagi, Y., Y. Yoshikai, K. Leggett, S. P. Clark, I. Aleksander, and T. W. Mak. 1984. A human T cell-  
754 specific cDNA clone encodes a protein having extensive homology to immunoglobulin chains.  
755 *Nature* 308: 145-149.

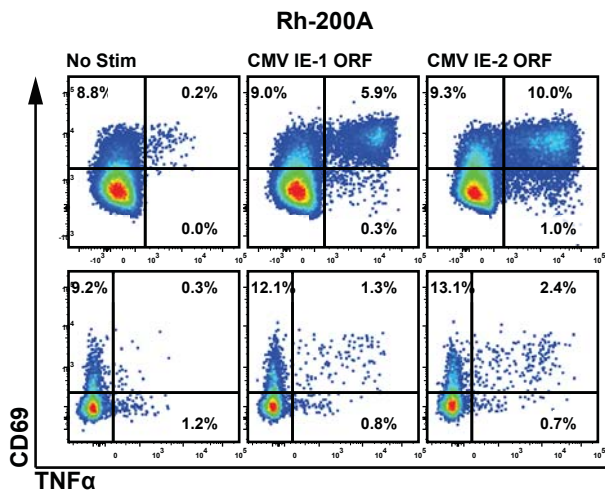
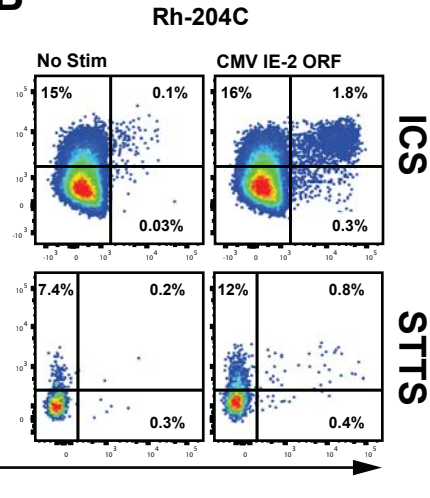
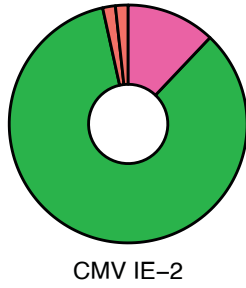
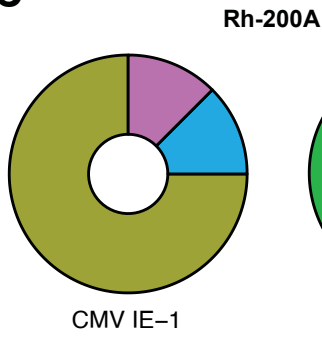
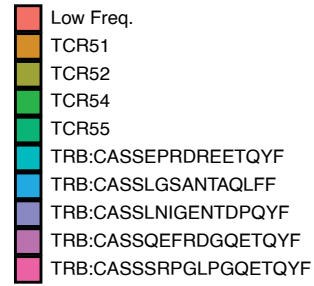
756 61. He, Q., X. Jiang, X. Zhou, and J. Weng. 2019. Targeting cancers through TCR-peptide/MHC  
757 interactions. *J Hematol Oncol* 12: 139.

758 62. Blum, J. S., P. A. Wearsch, and P. Cresswell. 2013. Pathways of antigen processing. *Annu Rev*  
759 *Immunol* 31: 443-473.

760 63. Sullivan, L. C., T. H. O. Nguyen, C. M. Harpur, S. Stankovic, A. R. Kanagarajah, M. Koutsakos, P. M.  
761 Saunders, Z. Cai, J. A. Gray, J. M. L. Widjaja, J. Lin, G. Pietra, M. C. Mingari, L. Moretta, J. Samir, F.  
762 Luciani, G. P. Westall, K. J. Malmberg, K. Kedzierska, and A. G. Brooks. 2021. Natural killer cell  
763 receptors regulate responses of HLA-E-restricted T cells. *Sci Immunol* 6.

764 64. Huard, B., and L. Karlsson. 2000. KIR expression on self-reactive CD8+ T cells is controlled by T-  
765 cell receptor engagement. *Nature* 403: 325-328.

766

**A****B****C****D****E**

Name	Alpha				Beta				
	CDR3a	V	J	C	CDR3b	V	D	J	C
<b>TCR51</b>	CATFSTDSWGKLF	TRAV17*01	TRAJ24*01	TRAC*01	CASTWGGANTAQLFF	TRBV5-6*01	TRBD1*01	TRBV5-6*01	TRBC1*01
<b>TCR52</b>	CAMRASSGGGYLTF	TRAV14-2*01	TRAJ6*01	TRAC*01	CASSEDRRNEKLFF	TRBV6-8*bw02	TRBD1*01	TRBJ1-4*01	TRBC1*01
<b>TCR54</b>	CAGRDNFNKFYF	TRAV25*01	TRAJ21*01	TRAC*01	CASSPREDSNYDYTF	TRBV27*w02	TRBD2*01	TRBJ1-2*01	TRBC1*01
<b>TCR55</b>	CVLRDYYGQNFIF	TRAV18*01	TRAJ26*w02	TRAC*01	CASSWRPDANYDYTF	TRBV27*01	---	TRBJ1-2*01	TRBC1*01